Contour inflections are adaptable features

Jason Bell — School of Psychology, University of Western Australia, Crawley, Australia; McGill Vision Research, Department of Ophthalmology, McGill University, Montreal, Quebec, Canada

Sinthujaa Sampasivam — School of Psychology, University of Ottawa, Ottawa, Ontario, Canada

David P. McGovern — Multisensory Cognition Group, Institute of Neuroscience, Trinity College Dublin, Dublin, Ireland

Andrew Isaac Meso — Institut de Neuroscience de la Timone, UMR 7289 CNRS & Aix-Marseille Université, Marseille, France

Frederick A. A. Kingdom — McGill Vision Research, Department of Ophthalmology, McGill University, Montreal, Quebec, Canada

An object's shape is a strong cue for visual recognition. Most models of shape coding emphasize the role of oriented lines and curves for coding an object's shape. Yet inflection points, which occur at the junction of two oppositely signed curves, are ubiquitous features in natural scenes and carry important information about the shape of an object. Using a visual aftereffect in which the perceived shape of a contour is changed following prolonged viewing of a slightly different-shaped contour, we demonstrate a specific aftereffect for a contour inflection. Control conditions show that this aftereffect cannot be explained by adaptation to either the component curves or to the local orientation at the point of inflection. Further, we show that the aftereffect transfers weakly to a compound curve without an inflection, ruling out a general compound curvature detector as an explanation of our findings. We assume however that there are adaptable mechanisms for coding other specific forms of compound curves. Taken together, our findings provide evidence that the human visual system contains specific mechanisms for coding contour inflections, further highlighting their role in shape and object coding.

Introduction

In mathematics, an inflection point is the point on a curve at which the gradient of the tangent, i.e., the curvature, changes sign. Under this definition, the stimuli in Figure 1 easily divide into contours that contain inflections and those that do not. Inflections are important descriptors in mathematics (Ewing, 1938; Irwin & Wright, 1917), linguistics (Faroqi-Shah & Thompson, 2007, 2010), and architecture/engineering (Chatila & Tabbara, 2004; Jahnkassim, 2002) in which contour inflections are known as "Ogee" curves. The importance of inflections for human vision is evidenced by the fact that contour inflections are not only ubiquitous features of natural scenes (Elder & Goldberg, 2002; Geisler, Perry, Super, & Gallogly, 2001), but they provide unique information about the shapes of objects (Bell, Hancock, Kingdom, & Peirce, 2010; Bertamini & Farrant, 2005; De Winter & Wagemans, 2008; Ivanov & Mullen, 2012; Mullen, Beaudot, & Ivanov, 2011) and the relations among edges (Singh & Hoffman, 1999). In addition, contour inflections along the 2-D silhouette of an object provide important cues to 3-D structure (Koenderink, 1984; Richards, Koenderink, & Hoffman, 1987). Despite their apparent importance, inflections have received little attention in models of shape and object coding, which have tended to focus on the role of oriented lines and curves (Barenholtz & Tarr, 2008; Carlson, Rasquinha, Zhang, & Connor, 2011; Connor, 2004; Hoffman & Richards, 1984; Pasupathy &

Citation: Bell, J., Sampasivam, S., McGovern, D. P., Meso, A. I., & Kingdom, F. A. A. (2014). Contour inflections are adaptable features. *Journal of Vision*, *14*(7):2, 1–14, http://www.journalofvision.org/content/14/7/2, doi:10.1167/14.7.2.

doi: 10.1167/14.7.2 Received December 10, 2013; published June 3, 2014 ISSN 1534-7362

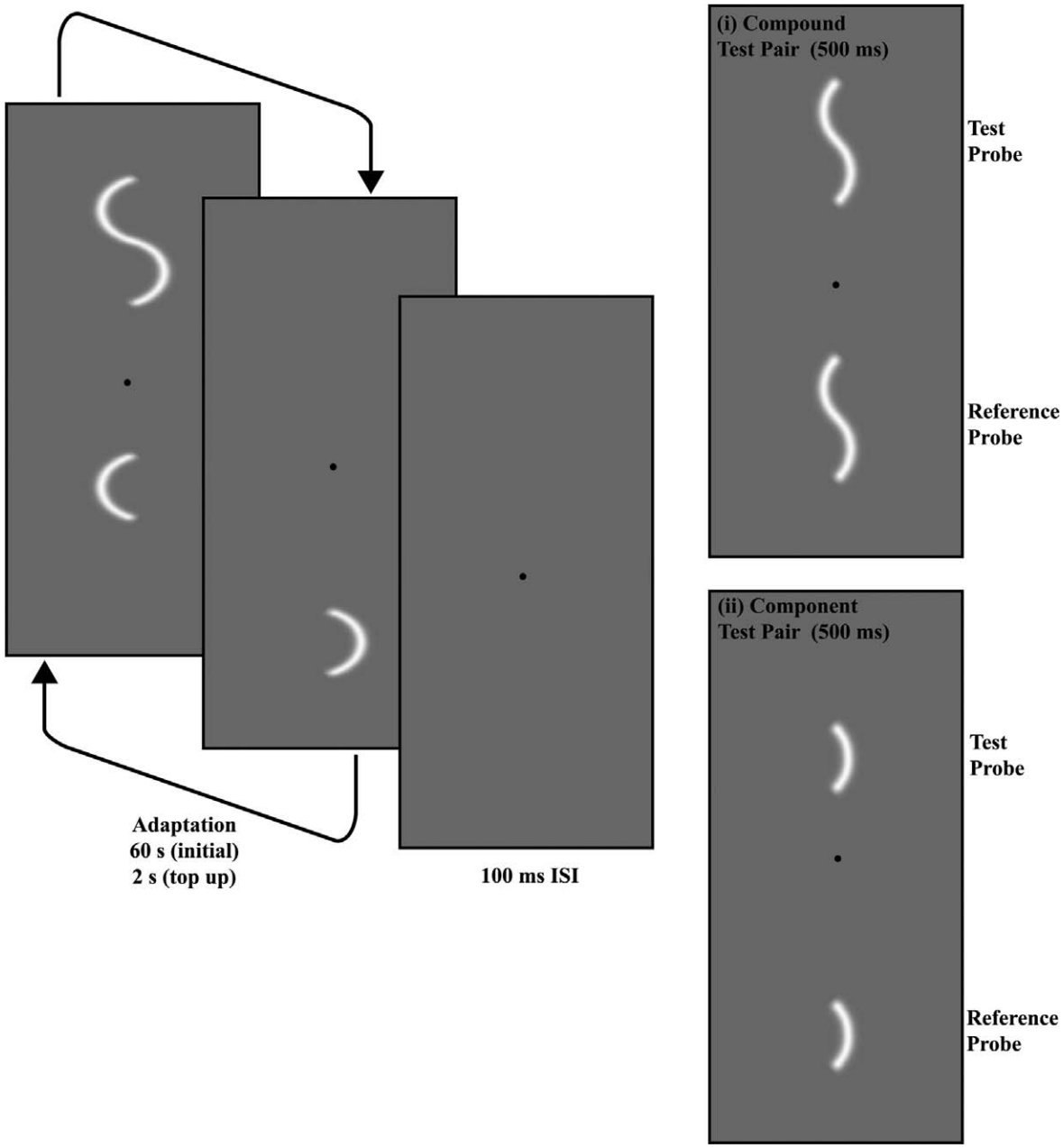

Figure 1. The illustration provides a schematic for the adaptation procedure used in Experiment 1A and 1B. During each 2 s of the adaptation period, the observer was presented with the Whole adaptor for 1 s in one visual hemifield and the two Parts adaptors, alternating in 1-s intervals, in the other hemifield. All adapting patterns had a sinusoidal modulation amplitude of 0.6°. Following 60 s of adaptation, the observer was presented with the test pair, either (i) Compound probes or (ii) Component probes. In each trial, the observer's task was to judge which probe had the higher perceived amplitude, i.e., deviated most from a straight line. The Reference probe amplitude was fixed at 0.2°, and the Test probe amplitude was varied according to a staircase procedure to obtain the PSE. A 2-s top-up adaptation period preceded each trial.

Connor, 2002; Poirier & Wilson, 2006, 2010; Yamane, Carlson, Bowman, Wang, & Connor, 2008). Models based on these features are popular because of the large body of evidence for specialized detectors in the cortex for oriented lines (Hubel & Wiesel, 1962, 1968; Kapadia, Westheimer, & Gilbert, 1999, 2000) and curves (Muller, Wilke, & Leopold, 2009; Pasupathy & Connor, 1999, 2001). Is there evidence for inflection coding mechanisms in the cortex? Neurophysiological studies of macaque monkeys have revealed subpopulations of neurons in visual area V4 (Pasupathy & Connor, 1999, 2001) and posterior inferotemporal

cortex (PIT) (Brincat & Connor, 2004, 2006; Yau, Pasupathy, Brincat, & Connor, 2010) that respond best to contour fragments containing inflections. In light of these findings, we ask whether the human visual system has mechanisms *specific* to coding contour inflections.

Our approach to this question is to consider whether a contour containing an inflection is processed by vision as a distinct shape as opposed to two oppositely signed curves. To decide between these two possibilities, we have used the method of compound adaptation (Hancock & Peirce, 2008; McGovern & Peirce, 2010; Peirce & Taylor, 2006) applied to a shape aftereffect, the phenomenon in which adaptation to a curved contour causes a less curved contour to appear even less curved (Bell, Gheorghiu, & Kingdom, 2009; Bell, Kanji, & Kingdom, 2013; Gheorghiu & Kingdom, 2006). The size of the aftereffect resulting from adaptation to a shape containing an inflection—the "Whole"—is compared to that from adaptation to the two temporally interleaved curves on either side of the inflection—the "Parts" (see Figure 1). The unique advantage of this method is that the Whole and Parts adaptors are equated for overall exposure, contrast energy, and curvature. If the adaptive effect of the Whole is greater than that of the Parts, this indicates that an additional mechanism, sensitive to the Whole and not just the Parts, has been adapted. Figure 1 provides an illustration of the experimental procedure.

This design is ideally suited to the study of inflections because the inflection is present in the compound curve, or Whole adaptor, but is not present in either of the two simple curves that form its Parts. For the purposes of this study, we consider a compound curve to be one containing multiple curvatures; the "S" shape contour in Figure 1 is an example but not the only one. By contrast, the single continuous nonclosed curves described by the component curves in Figure 1 are examples of simple curves. Mechanisms for simple curves have been extensively studied; mechanisms for specific forms of compound curves, such as the contour inflection, have not.

In our first experiment, we show that human observers display a specific aftereffect to a shape containing an inflection. Subsequent experiments show that the aftereffect cannot be explained on the basis of the procedure itself or by adaptation to the component curves that make up the shape—the inflection needs to be present. We further demonstrate that the inflection aftereffect is selective for the luminance polarity relationship between adaptor and test, a finding that is inconsistent with the argument that our aftereffect is based on simple orientation adaptation. Next, we show that the contour inflection aftereffect does not transfer to a contour inflection with an opposite sign of amplitude modulation but does transfer to a symmetrical counterpart with the same primary axis of orientation, suggesting a special role for symmetry in the coding of contour inflections. Finally, we show that inflection adaptation transfers weakly to a compound curve that does not contain an inflection, ruling out a general compound curvature detector as an explanation of our findings. In relation to this final point, we go on to show that there are adaptable mechanisms for other specific forms of compound curves but not for all compounds.

Materials and methods

Participants

Eight experienced psychophysical observers participated in the current study. Three were female, and five were male. Four were naïve as to the experimental aims, and observers JB, AM, SS, and DM were authors. At least two naïve observers participated in each experiment. All reported normal or corrected-to-normal visual acuity. Participation was voluntary and unpaid. The research protocol was approved by the McGill University Human Research Ethics committee and, thus, has been conducted in accordance with the principles of the Declaration of Helsinki.

Apparatus and stimuli

Stimuli were created using Matlab version 7.6 and loaded into the frame-store of a Cambridge Research Systems ViSaGe video-graphics system. Stimuli were presented on a Sony Trinitron G400 monitor with a screen resolution of 1024 × 768 pixels and a refresh rate of 100 Hz. The luminance of the monitor was calibrated using an Optical OP200-E (Head Model #265). The mean luminance of the monitor was 50.4 cd/m^2.

Example test stimuli are shown in Figure 1. Unless otherwise specified, each Whole inflection shape consisted of one full cycle of sinusoidal shape modulation along a vertical line. Each Part component consisted of one half cycle of sinusoidal modulation along a vertical line. A contrast smoothing function was applied to both ends of the contours, ensuring that the contrast energies of the Whole and summed Parts were identical as were the curvature represented by the Whole and interleaved Parts adaptors. The cross-sectional luminance profile of each contour was a Gaussian with sigma of 0.085°.

Experiment 1 procedure

Whole versus Parts

Participants were adapted to contour inflections in two regions of the visual field, centered 3° above and below a fixation dot. The procedure is shown schematically in Figure 1. In one visual hemifield, the inflection contour was presented as a complete shape (Whole condition) and in the other as two parts presented in alternation (Parts condition). All patterns had a sinusoidal modulation of shape with a shape amplitude of 0.6°. Exposure was equated in the two hemifields by presenting the Whole shape for half of the time (1 s out of every 2 s), interleaving with a blank gray screen, whereas the Part stimuli alternated every 1 s. The temporal phases of the alternations in each hemifield were independently randomized so that no coherent motion was observed. The position of the stimulus was also randomized ±0.25° every 2 s (i.e., after each presentation of all stimuli) in order to reduce adaptation to local position and orientation.

The initial period of adaptation lasted for 60 s and was "topped-up" with another 2 s of adaptation prior to each trial. This was followed by a 100-ms interstimulus interval, consisting of a mean gray screen, before presentation of the probe stimuli for 500 ms. A central fixation spot was visible for the entire trial. After the adaptation period, a probe stimulus was presented in each of the two adapted locations. The observer was instructed to select whether the upper or lower probe appeared to be greater in amplitude, i.e., which deviated most from a straight line. The probes (shown on the right-hand side of Figure 1) could either be a pair of inflection contours (Compound test pair) or a pair of component curves (Component test pair). One of each test pair, the reference probe, was presented in the Parts adaptor field and had a fixed amplitude of 0.2°. The other, the test probe, was presented in the Whole adaptor field and varied in amplitude via a one-down, one-up staircase. In the first trial, the amplitude of the test probe was set to a random ratio of reference probe amplitude between 0.5 and 1.5. Following each response (a key press), the computer adjusted the amplitude of the test probe in a direction opposite to that of the response, i.e., toward the point of subjective equality (PSE) with the reference probe. For the first six trials, the amplitude was adjusted by a factor of 1.12 and thereafter by a factor of 1.06. Each run was terminated after 25 trials, and the PSE was calculated as the geometric mean ratio of test pattern amplitudes over the last 20 trials, which, on average, contained six to 10 reversals. Typically, eight PSEs were measured for each condition. In half of the sessions, the Whole adapting pattern was in the upper visual hemifield whereas, in the other half of the sessions, the Parts adapting pattern was in the upper visual hemifield. In addition, we measured the PSE in sessions containing no adaptation stimuli; these served as baselines and provided a measure of any visual field biases. The size of the aftereffect calculated for each session was given by the percentile difference in the amplitudes of the test pair (reference probe divided by test probe) at the PSE minus the same PSE value without adaptation: These preadaptation and postadaptation PSE values are the point of comparison for the repeated measures t tests reported below. The mean ±1 standard errors (SE) of these values across sessions are the points shown in all the graphs.

Experiment 2 procedure

Tilt aftereffect

In conditions measuring the tilt aftereffect (TAE), the adapting stimuli were a pair of lines with one line presented 3° above fixation at an orientation of 10° and the other line presented 3° below fixation at an orientation of −10°. Test lines were presented in the same positions as the adaptors, and the observer was instructed to judge which line appeared to be rotated furthest clockwise from vertical. The PSE was calculated as the mean angular difference in orientation between the upper and lower lines across the last 20 trials.

Inflection aftereffect

In conditions measuring the inflection aftereffect (IAE), adapt and test stimuli were pairs of Whole inflection stimuli; see Figure 3A inset for opposite luminance polarity examples of adapt and test stimuli described below. In one visual hemifield, the observer was presented with a steep inflection adaptor (high amplitude: A = 0.27°) and, in the other visual hemifield, a shallow inflection adaptor (low amplitude: A = 0.09°). The test pair was presented in corresponding locations, at the geometric mean amplitude of the adapting pair (A = 0.16°), plus or minus a random amount in the first trial. During adaptation, the positions of both adaptors were randomly jittered every 500 ms by ±0.25°. The test procedure was the same as that reported in the Parts versus Whole paradigm above with the exception that, for the IAE, the reference probe was not fixed in amplitude; instead both test patterns were varied depending on the observer's response. By allowing both tests to vary in amplitude during the trials, we are measuring the absolute size of the aftereffect rather than the difference in the adaptive strength of the two adaptors. The size of the IAE calculated for each session was given by the percentile difference in the amplitudes of the test pair (reference probe divided by test probe) at the PSE minus the same PSE value without adaptation.

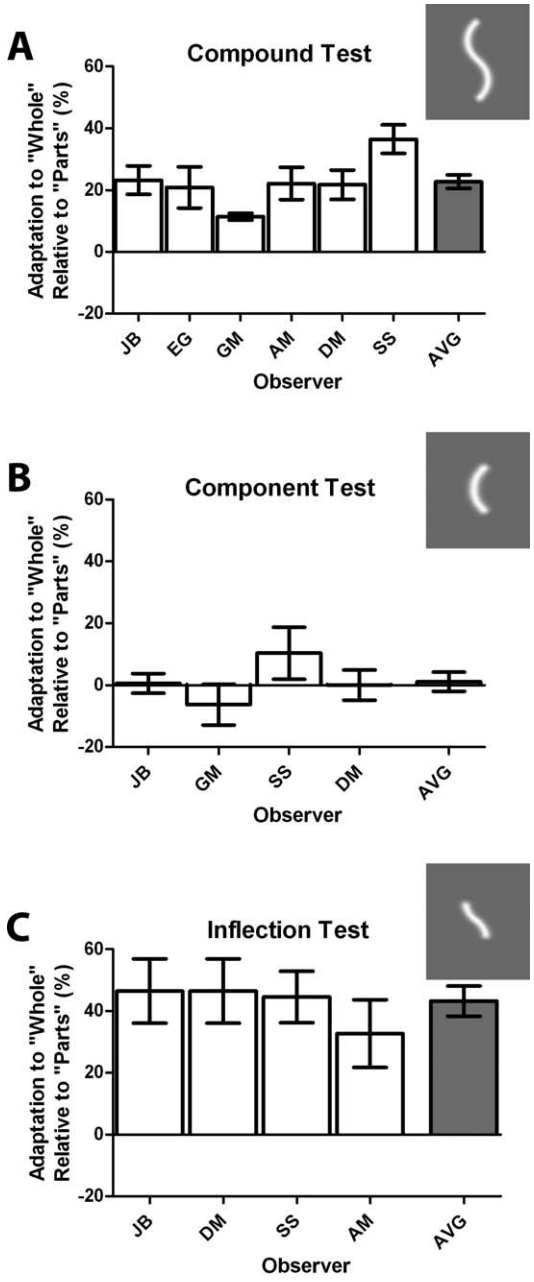

Figure 2. Whole versus Parts experimental data. (A) Compound data: results for six observers, showing the percentage difference in the size of the aftereffect produced by the Whole and Parts adaptors with a Compound test, i.e., a pair of inflection contours as shown in the inset. The gray bar here (and for B and C) shows the mean difference across observers. Because this result is the principal finding of our study, we tested several additional naïve observers in these conditions. (B) Component data: results for four observers using the same adaptation procedure but with single-sign curve tests, i.e., one half of the compound test as shown in the inset. (C) Inflection data: results for four observers using the same adaptation procedure, but now the Whole and Part stimuli have been shortened by half to better represent a contour inflection as shown in the inset. Data presented in all figures show the mean ± 1 *SE*.

Results

Experiment 1: Contour inflections are adaptable features

In order to determine whether an inflection is an adaptable feature, we compare the magnitude of adaptation to a Whole contour containing an inflection to its two temporally interleaved Parts, cut at the point of inflection. If the adaptive effect of the Whole is greater than that of the Parts, this indicates that an additional mechanism, sensitive to the Whole, has been adapted.

Figure 2 shows the size of the aftereffect measured in the visual hemifield containing the Whole adaptor relative to that in the hemifield containing the Parts adaptor. The amplitude difference is shown in percentage terms with positive values indicating greater adaptation to the Whole. In Figure 2A, data is shown for conditions in which the test pair were line contours containing inflections (see figure inset). Bearing in mind that a score of zero would indicate that adaptation to the Whole and Parts adaptors produced the same sized aftereffect, the results show that the Whole adaptor produced, on average, a 20% larger aftereffect than the Parts adaptor (gray column). The difference is highly significant, $t(43) = 7.33$, $p < 0.0001$ (one-tailed), and shows that, in addition to curvature adaptation (which occurs equally for Whole and Parts adaptors), an additional mechanism sensitive to the inflection in the Whole was adapted.

Could our results be an artifact of procedure? Although our method ostensibly equates the contrast energies and curvatures of the Whole and Parts adaptors across each 2-s epoch, it would seem prudent to test whether any unforeseen stimulus differences were responsible. Therefore we reran the experiment using test probes consisting of a pair of single curves, i.e., with no inflections (see Figure 2B inset). If the stronger aftereffect produced by the Whole adaptor is simply due to an unforeseen difference in contrast energy or curvature, then it should not matter whether the test probe contains an inflection or not. Results are shown in Figure 2B. In contrast to the previous data set, all observers scored zero or close to zero, indicating that there is no difference in the size of the aftereffect obtained from Whole and Parts adaptors, $t(31) = 1.45$, $p = 0.15$. Thus it is highly unlikely that our initial finding is an artifact of contrast energy or curvature.

Do our results demonstrate selective adaptation to the inflection component of the shape or simply to a compound "S" shape? To better isolate the contour inflection, we reduced our Whole inflection contour by half to a half cycle centered on the inflection point (see Figure 2C inset). There is, of course, a limit to how far

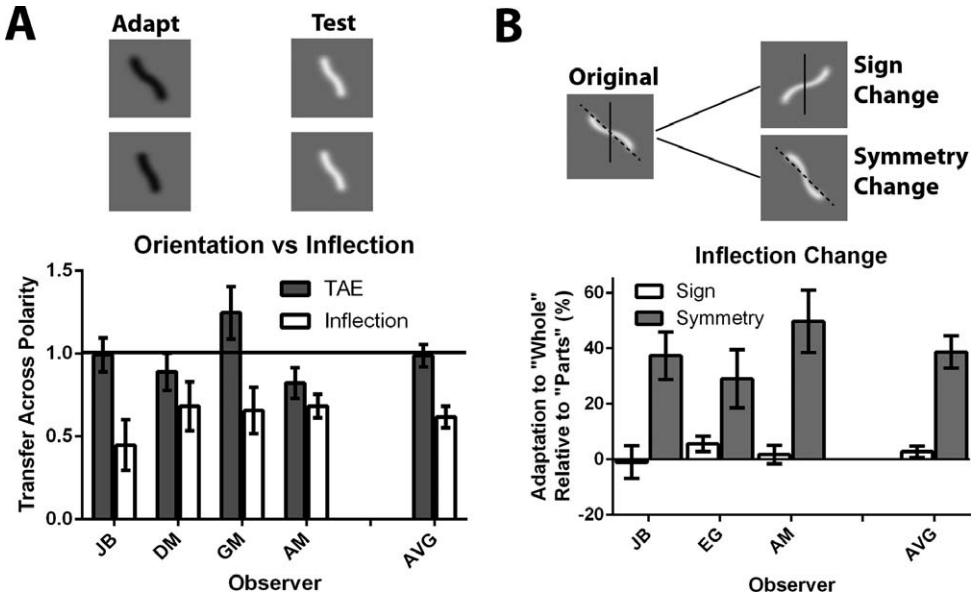

Figure 3. (A) Opposite polarity control: results for four observers, showing the transfer of aftereffect across opposite-luminance-polarity adaptor and test for the TAE (gray bars) and IAE (white bars). Examples of opposite polarity adapt and test stimuli for the IAE condition are shown in the inset. Transfer was computed as the ratio of same to opposite polarity, with one indicating complete transfer and zero no transfer. (B) Sign transfer data: results for three observers using the Parts versus Whole adaptation procedure and when the test pair was either opposite sign/amplitude phase (white bars) or symmetrical counterparts (gray bars) to the adapting patterns. The figure inset depicts each of these manipulations. The solid line shows a sign change or flip about the vertical axis, and the dashed line shows a change along the primary axis of symmetry: diagonal. As in Figure 2, the data are represented as the percentage difference in the size of the aftereffect produced by the Whole and Parts adaptors. Data presented in all figures show the mean $\pm$ 1 *SE*.

one can shorten the contour: Although the inflection is a single point, it can only be realized at the junction of two oppositely signed curvatures. We suggest that the stimulus shown in the inset of Figure 2C (and the top row of Figure 3) is a simple and concise example of a contour inflection. We reran the Parts versus Whole experiment using this shortened contour. Thus, as before, the curvature and contrast energies of the Parts and Whole adaptors were the same across each 2-s epoch. The test pair was a low amplitude pair of the shortened inflection contours (see Figure 2C inset). All other aspects of the testing procedure (e.g., amplitudes and durations) were unchanged.

Figure 2C shows the results for four observers (clear bars) and their average (gray bars). All observers recorded a larger aftereffect in the visual hemifield corresponding to the Whole adaptor than in the hemifield corresponding to the Parts adaptor. The difference is highly significant, $t(29) = 7.07$, $p < 0.0001$ (one-tailed). These findings are consistent with selective adaptation of a mechanism selective for a contour containing an inflection. Moreover, these data replicate our original finding (Figure 2A) using a stimulus that (a) more concisely represents a contour inflection and (b) poorly represents any more elaborate compound shape. This simplified contour inflection stimulus is now used in subsequent experiments. Next, we assess the role of orientation adaptation in the contour IAE.

Experiment 2: Inflection or orientation?

We have shown that our aftereffect cannot be explained on the basis of contrast or curvature adaptation. However, there is another possibility. The Whole adaptor contains a short length of oriented contour around the inflection point not present in the Parts adaptor; could this cause the greater aftereffect? To test this possibility, we exploited the fact that orientation adaptation, as measured by the well-known TAE (Gibson & Radner, 1937), is insensitive to luminance polarity (Magnussen & Kurtenbach, 1979), a finding that we verify below. If orientation adaptation underpins the inflection-specific component of the aftereffect, then the aftereffect should be similarly agnostic to luminance polarity. On the other hand, if contour inflections are processed at intermediate stages of the form pathway (Brincat & Connor, 2004, 2006; Pasupathy & Connor, 1999, 2001, 2002; Yau et al., 2010), then, like other intermediate-stage shape aftereffects, such as curvature and global shape aftereffects (Bell, Gheorghiu, Hess, & Kingdom, 2011; Bell & Kingdom, 2009; Gheorghiu & Kingdom, 2006; Han-

cock, McGovern, & Peirce, 2010), it should be luminance-polarity selective. Our procedures for measuring both the TAE and IAE are described in Materials and methods.

Figure 3A shows results for four observers and for the two types of stimuli (gray bars for the TAE, white bars for the IAE). The rightmost bars show the average of all observers. Each bar plots the magnitude of aftereffect for a dark (negative luminance polarity) adaptor and bright (positive luminance polarity) test as a proportion of the size of the same aftereffect measured when the adaptor and test patterns are both bright. This condition is depicted in the figure inset for the IAE. A value of 1.0 on the vertical axis indicates that the aftereffect for same and opposite luminance polarity conditions is equal, and a value smaller than one indicates selectivity for luminance polarity. Consistent with previous research (Magnussen & Kurtenbach, 1979), TAE transfer ratios across luminance polarity are approximately one (average: 0.98), indicating no selectivity for luminance polarity. For the IAE data, however, the same observers all display transfer ratios that are consistently smaller than one (average: 0.61) and systematically smaller than their own comparative transfer for the TAE. The incomplete transfer of the IAE indicates a selectivity for luminance polarity similar to that found for other intermediate-stage shape encoders (Bell et al., 2011; Bell & Kingdom, 2009; Gheorghiu & Kingdom, 2006; Hancock et al., 2010). The difference in luminance polarity selectivity between the TAE and IAE data is significant, $t(15) = 3.23$, $p = 0.0028$ (one-tailed). Because inflection adaptation is tuned for an attribute (luminance polarity) that orientation adaptation is not, it seems unlikely that our contour inflection aftereffects result from local orientation adaptation.

Experiment 3: Sign selectivity of the inflection coding mechanism

We have demonstrated a specific aftereffect for a contour inflection. Next, we examined whether inflection adaptation is selective for the sign of a contour inflection. This is akin to asking whether mirror symmetry is important for the processing of inflection contours as it is for simple curves (Bell et al., 2009) and for particular objects (Rhodes et al., 2007; Wilkinson & Halligan, 2002). To test for selectivity, we reran the Whole versus Parts conditions from Experiment 1 but reversed the sign of the shape-amplitude modulation of the compound test pair while leaving the adapting patterns unchanged (see Figure 3B inset for an example of a sign change). Our contour stimuli are modulated relative to a vertical line, and so, for our stimulus, a sign change is equivalent to a flip around the vertical axis as shown in the inset in Figure 3B, labeled "sign change." The solid line here depicts the axis around which this stimulus has been flipped. Using an analogous manipulation, two of the authors have previously shown that curvature aftereffects do transfer across a change in sign or to opposite phase (Bell et al., 2009), and we have also verified that the transfer to opposite sign curves is replicated using the Whole versus Parts procedure (Bell, Sampasivam, McGovern, & Kingdom, 2010). Therefore, we predicted a similar result here, namely a score greater than zero, indicating that Whole inflection adaptation has transferred to an opposite sign test.

The white bars in Figure 3B show the results for the opposite sign conditions. Contrary to our prediction, for all three observers, data values are close to or at zero, indicating no Whole adaptor advantage. The rightmost white bar plots the average of all observers. A paired samples t test found no difference in the size of the aftereffect in each field, $t(11) = 1.37$, $p = 0.19$. Our finding demonstrates that IAEs do not transfer to opposite sign contours, indicating that inflection coding is selective for the sign of the contour inflection.

As noted previously, curvature adaptation has been shown to transfer strongly across opposite sign adapt and test pairs (Bell et al., 2009), and this finding was presented as evidence for the existence of sign-invariant curvature processing mechanisms, ones likely used in processing symmetry. In contrast, the current results suggest that the IAE is selective for the sign of the adaptor. Of course, changing the sign of amplitude modulation creates a mirror-symmetric version of an inflection with respect to the two cardinal axes. However, it could be argued that the most similar mirror-symmetric counterpart to the contour inflection is one that is flipped about its primary axis of orientation rather than reversed in sign. This primary axis is denoted in the inset of Figure 3B by the dashed line. Thus, reversing the sign of amplitude modulation creates an intuitively symmetrical version of a curve but not so a contour inflection (see Figure 3B inset, solid and dashed lines depict each axis of change). Therefore we reran our experiment using a pair of contour inflections that were mirror-symmetric about the major axis of orientation of the contour (for simplicity, we labeled this "symmetry change" in Figure 3B) as tests. All other aspects were unchanged. The same three observers now interestingly obtain values greater than zero (Figure 3B, gray bars), indicating a Whole adaptor advantage. The rightmost gray bar plots the average of all observers. The difference was significant, $t(17) = 6.27$, $p < 0.0001$ (one-tailed), showing that adaptation to a whole contour inflection transfers completely to a mirror-symmetric version of itself. This complements previous reports of a special role of mirror symmetry in the processing of parts of shapes (Bell et al., 2009).

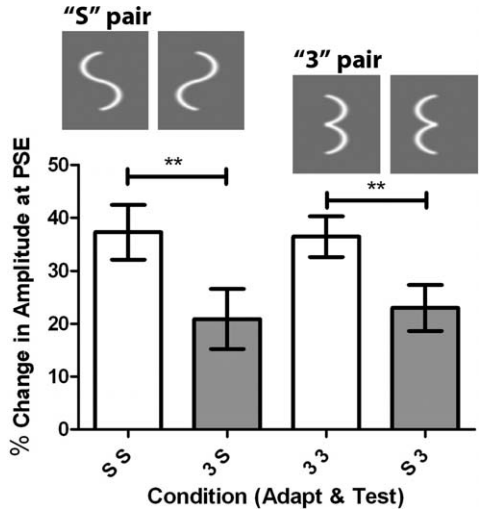

Figure 4. Compound curve versus inflection data. The vertical axis plots the percentile difference in amplitude between the two test patterns at the PSE. On such a scale, zero equals no adaptation. The horizontal axis describes the adapt and test combination. The adaptor type is listed first and the test second. White bars show conditions in which adapt and test are the same type, gray bars in which they are different. The data plotted in each column is the average for three observers. Error bars show mean $\pm$ 1 *SE*. The horizontal lines show the specific comparison relevant to this experiment. ** $p < 0.01$. Figure insets illustrate the appearance of each adapting pattern in its pair.

Finally, Experiment 3 provided an additional control for our Whole versus Parts procedure. Although the Whole adaptor advantage was shown not to occur for a Parts test pair (single curves, Figure 2B), it is possible that the Whole adaptor advantage for compound tests was due to the similarity between adapt and test patterns rather than due to the presence of the inflection in the Whole. That is, in all compound test conditions to date, adapt and test are both whole contour inflection shapes and are both the same vertical length. Of course, if this similarity were to underpin our findings, then one would predict that the Whole adaptor advantage would be obtained whenever we use a compound test regardless of the sign difference between adapt and test. The results in Figure 3B (white bars) show that this is not the case: The Whole adaptor advantage was abolished when adapt and test were of opposite sign.

Experiment 4: Inflection or compound curve?

So far, the evidence supports a mechanism that is selective for a contour inflection. However, an inflection only exists as part of a compound curve, i.e., at the junction of two oppositely signed curves. This begs the question: Do our results implicate a mechanism that is specific to inflections or one generally responsive to compound curves? To test between these two possibilities, we ran an experiment in which we measured aftereffects using two types of compound curve. Both compounds were constructed from the same two component curvatures, but one contained an inflection, and the other did not. The inflection compound was an "S"-shaped contour, and the noninflection compound was constructed by reversing the sign of one of the two curves in the "S," which maintained the component curves but eliminated the change in the sign of curvature along the contour. We characterize the no-inflection adaptor as a "3." Figure 4 shows examples of both types of pattern. We acknowledge that the two compounds differ in their representation of a third feature: an inflection in the "S" compound and an additional acute curvature in the "3" compound. However, the question here is whether the spatial arrangement of the two-component curvature is important. The answer should be "yes" if inflections represent a specific type of compound and "no" if our results are attributable to a general compound detector sensitive to these two component curves.

During adaptation, the compound, whether an "S" or a "3," alternated every 1 s with its opposite sign partner, i.e., a backward "S" or backward "3." This meant that observers viewed the same component curves, both above and below the midpoint of each compound, during adaptation: If summed across a 2-s adaptation period, each condition represented the same figure eight–shaped contour. The tests were either a pair of "S" contours or a pair of "3" contours with one of each pair, the test probe, presented in the unadapted visual hemifield. Unlike in Experiments 1 and 3, the adaptor was presented to only one hemifield, meaning that we measured the absolute size of the aftereffect rather than its relative size in the two hemifields. Across runs, the adaptor was presented an equal number of times to the upper or lower visual field, and as in previous experiments, the adaptor was initially presented for 60 s with a 2-s top up between test trials. The percentile difference in amplitude between the two patterns at the PSE is plotted in Figure 4. PSEs for runs in which no adaptor was presented were subtracted in order to remove visual field biases from the aftereffects reported. Therefore, in this data, a score of zero would indicate no adaptation.

If compound shapes containing two oppositely signed curves are processed by a specific subset of compound shape mechanisms, adapting to an "S" pair should produce a larger aftereffect in an "S" than a "3" test, and adapting to a "3" pair should produce a larger aftereffect in a "3" than an "S" test. By contrast, similarly sized aftereffects across all four conditions

would be expected if the stimuli were processed by a general compound curvature mechanism.

Figure 4 presents the averaged results for three observers in all four conditions. The vertical axis describes the size of the measured aftereffect (the perceived decrease in modulation amplitude) in percentage terms. The horizontal axis describes the condition with adaptor type followed by test type. Conditions showing same and different adapt/test combinations are shown in white and gray, respectively. Aftereffects are larger in same adapt/test compared to different adapt/test conditions. A one-way repeated-measures ANOVA confirmed that adaptor test pairing had a significant effect on the size of the aftereffect, $F(3, 11) = 9.86$, $p < 0.0001$. Bonferroni post hoc comparisons (corrected for multiple comparisons) confirmed there was a significant difference between same and different pairings ("S" pair adapt "S" test significantly greater than "3" pair adapt "S" test, $t = 4.2$, $p < 0.01$; "3" pair adapt "3" test significantly greater than "S" pair adapt "3" test, $t = 3.45$, $p < 0.01$).

Experiment 4 was designed to test whether the spatial arrangement of the two component curves was important. Clearly the answer is "yes." In addition, the strong adaptation to the "3" compound shape indicates that there are adaptable mechanisms for compound curves that do not describe an inflection. This is an important point that we will return to in the Discussion. Taken together, however, our data are consistent with the idea that distinct mechanisms are adapted by the two different combinations of the two component curves: one selective for the compound shape containing the inflection and another selective for the compound shape containing the cusp.

Experiment 5: No Whole adaptor advantage for a locally processed stimulus

Despite controls provided in this and other studies using the Whole versus Parts approach (Bell, Hancock, et al., 2010; McGovern, Hancock, & Peirce, 2011; McGovern & Peirce, 2010; Peirce & Taylor, 2006), the concern remains that the Whole adaptor advantage is simply due to the greater spatiotemporal similarity between Whole adaptor and Whole test compared to Parts adaptor and Whole test. One way to test for such a possibility is to employ a stimulus that does not involve feature integration, i.e., that does not involve global processing. A well-known example of a locally processed stimulus is the high radial-frequency (RF) pattern (Wilkinson, Wilson, & Habak, 1998). RF patterns are created by sinusoidally modulating the radius of a closed contour. Some of us have previously used the Whole versus Parts paradigm to demonstrate global processing of a suprathreshold amplitude low RF pattern (RF4) (Bell, Hancock, et al., 2010). It is widely accepted that, for RF patterns containing more than 10 cycles (RF10), there is no global pooling of information as evidenced by probability summation across local feature detection (Bell & Badcock, 2009; Bell, Badcock, Wilson, & Wilkinson, 2007; Jeffrey, Wang, & Birch, 2002; Loffler, Wilson, & Wilkinson, 2003). We chose an RF15 pattern, which is 50% above this global threshold. The luminance profile of the RF15 pattern was a D4 with a peak spatial frequency of 8 cpd and pattern contrast was set to its maximum ($C = 0.99$), consistent with previous research (Wilkinson et al., 1998).

The predictions for this experiment are as follows: If the Whole versus Parts difference arises due to the spatiotemporal similarity of adaptor and test, then we should observe a larger aftereffect in the visual field corresponding to the Whole adaptor. This would be evidenced by values greater than zero in the results below. However, values of zero would indicate no Whole adaptor advantage, ruling out the above arguments. In short, a score of zero would validate the method, and a score greater than zero would imply the Whole adaptor advantage is an artifact of procedure.

The Whole versus Parts procedure for the RF experiment has been described elsewhere (Bell, Hancock, et al., 2010) and is essentially analogous to the procedure employed in this study. The major points are summarized as follows, and a schematic of the procedure is shown in the inset of Figure 5. RF15 stimuli were cut into four segments to create the Part adaptors. A smoothing function was employed to avoid orientation cues at the ends of the parts. Critically, the contrast energy of the four Part adaptors when summed is equal to that of the Whole adaptor. During adaptation, in one visual hemifield, each Part adaptor is presented in isolation for 500 ms, meaning all parts are temporally interleaved in random order every 2 s. In the opposite visual hemifield, the Whole adaptor is presented for 500 ms in total, presented at a random point in the 2-s sequence. Thus, as before, the critical feature is that the total exposure to the Part and Whole adaptors is identical across the adaptation (60 s) and top-up (2 s) phases of the procedure. To maximize the possibility of local orientation and position adaptation, the phase and position of the adaptor and test were synchronized and not jittered across the run. As before, the test contained one fixed amplitude whole RF15 pattern, and the reference contained an adjustable whole RF15 test in the other visual hemifield, i.e., the probe. The amplitudes of the Whole and Part adaptors, expressed as a proportion of the mean 1° radius of the pattern were double (0.1) that of the fixed reference (0.05), consistent with our previous work using this procedure for low RF patterns (Bell, Hancock, et al., 2010). The observer's task in each trial was to choose

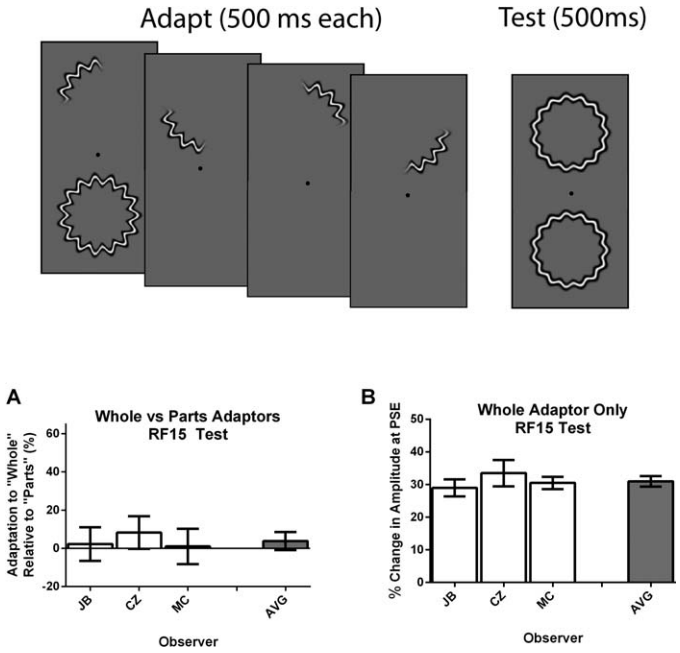

Figure 5. Inset: The illustration provides a schematic for the adaptation procedure used in Experiment 5. During each 2 s of the adaptation period, the observer was presented with the Whole adaptor for 500 ms in one visual hemifield and the four Parts adaptors, alternating in 500-ms intervals, in the other hemifield. All adapting patterns had a sinusoidal modulation amplitude of 0.1 expressed as the proportion of radius modulation on a 1° radius RF15 pattern. Following 60 s of adaptation, the observer was presented with the test pair. In each trial, the observer's task was to judge which probe had the higher perceived amplitude, i.e., deviated most from a straight line. The Reference probe amplitude was fixed at an amplitude of 0.05, and the Test probe amplitude was varied according to a staircase procedure to obtain the PSE. A 2-s top-up adaptation period preceded each trial. (A) Whole versus Parts experimental data. Results for three observers, showing the percentage difference in the size of the aftereffect produced by the Whole and Parts adaptors with an RF15 test. The rightmost gray bar shows the mean difference across observers. (B) Whole adaptor only experimental data. Results for three observers showing the size of the amplitude aftereffect on an RF15 test due to the RF15 adaptor. The rightmost gray bar shows the mean across observers. Data presented in both figures show the mean ± 1 *SE*.

the pattern that appeared higher in amplitude (had greater bumps). The test procedure was otherwise identical to that described in the Whole versus Parts procedure for inflections in the general Materials and methods. Again, the size of the aftereffect calculated for each session was given by the percentile difference in the amplitudes of the test pair (reference probe divided by test probe) at the PSE minus the same PSE value without adaptation: These preadaptation and post-adaptation PSE values are the point of comparison for the repeated measures *t* tests reported below. The mean ±1 standard errors (*SE*) of these values across sessions are the points shown in all the graphs.

Figure 5A presents the Whole versus Parts experimental data for three observers (two naïve). The rightmost gray bar shows the average of the three. For all three observers, the values are at or approximately zero. This indicates no difference in the adaptive strength of the Whole relative to the Parts. A one-tailed paired samples *t* test confirmed that there was no significant difference between PSEs for baseline no-adaptor trials and adaptor trials, $t(11) = 0.98$, $p = 0.17$. This suggests that there is no Whole adaptor advantage for a stimulus that does not involve integration of features as in an RF15 pattern.

This conclusion, however, is predicated on there being strong and measurable aftereffects to our adapting stimuli: Note that the Whole versus Parts method measures relative, not absolute, adaptation effects. To verify that there was significant adaptation, we removed the Part adaptors from the sequence and repeated the trials with a blank screen instead. This directly measures the size of the aftereffect obtained from the Whole RF15 adaptor. Now a value greater than zero indicates an amplitude aftereffect due to the RF15 adaptor. Figure 5B shows results in this condition for the same three observers. Again, the rightmost gray bar indicates the average of all observers. Clearly, there is a large and significant amplitude aftereffect on the RF15 test due to the Whole RF15 adaptor, $t(11) = 9.2$, $p < 0.0001$. The direction of this aftereffect is repulsive; that is, there is a perceived reduction in pattern amplitude following adaptation to a higher amplitude pattern. This repulsion is consistent with earlier data using globally processed low RF patterns (Bell et al., 2011; Bell, Hancock, et al., 2010; Bell & Kingdom, 2009). Critically, this large and significant aftereffect demonstrates that the lack of a Whole adaptor advantage in Figure 5A is not simply due to a lack of adaptive strength for either the Whole or Part adaptors.

In summary, Experiment 5 shows that the Whole adaptor advantage, as measured by the Whole versus Parts procedure, does not occur for stimuli that are known to be processed locally. Moreover, the result is not due to a lack of overall adaptation and, crucially, was obtained using a procedure identical to that for which a Whole adaptor advantage *was* found when a low RF pattern was employed (Bell, Hancock, et al., 2010). This finding is important because it demonstrates that, although there are adaptable mechanisms for specific forms of compound shape, these mechanisms do not extend to arbitrarily complex contours, such as RF15.

Discussion

To summarize, we have demonstrated an aftereffect that

- Is selective for a contour containing an inflection (Figure 2A)
- Is not simply due to adapting to the component curves of the contour inflection (Figure 2B)
- Is maintained for a shortened, concise example of an inflection that poorly represents a more elaborate compound shape (Figure 2C)
- Is not simply due to adapting to the local orientation at the point of inflection (Figure 3A)
- Transfers strongly to a mirror-symmetric counterpart to an inflection but *does not* transfer to an inflection with an opposite sign (Figure 3B)
- Cannot be explained by the existence of a general compound curvature detector (Figure 4)
- Is not due to the procedure; the Whole versus Parts procedure correctly failed to produce a Whole adaptor advantage for a locally processed stimulus (Figure 5)

On the basis of these findings, we argue that contour inflections are adaptable features of the human visual system. Of course, a contour inflection only exists as part of a compound curve, so it is a sine qua non that our study should set out to determine whether an aftereffect obtained by adaptation to a compound curve containing an inflection implicated an inflection-specific mechanism as opposed to one sensitive to compounds in general. In Experiment 4, we found that "S"-shaped adaptors produced larger aftereffects in "S"-shaped tests than did "3"-shaped adaptors and vice versa in spite of the fact that, during adaptation, the same set of component curves, both above and below the midpoints of the compounds, were presented. In the third part of Experiment 1, we also demonstrated that the IAE was not affected by a reduction in the compound shape. Here, we took a compound curve "S" shape and reduced its overall length by half. The resulting stimulus contained an inflection but was an impoverished example of a multicurve compound (see Figure 2C inset). Because local curvature adaptation for the Parts and Whole adaptors is always identical (Figure 2B), the prediction for this configuration was that a compound-curvature mechanism would be only weakly adapted by such a stimulus and that, therefore, the measured aftereffect would be relatively small. An inflection-coding mechanism, on the other hand, would be strongly adapted by this shortened stimulus, and so there should be no reduction in aftereffect. This is what happened (compare Figure 2A and 2C).

The reader may note from this comparison that the aftereffect for the shortened stimulus configuration increased compared to that from the original "S" shape. Why the increase? Previous work has shown that curvature adaptation is suboptimal when the length of a curve is reduced below one half cycle of modulation: a simple curve (Gheorghiu & Kingdom, 2007). Consequently, it seems likely that the curvature adaptation in our shortened inflection stimulus was suboptimal. However, this reduction affected the Whole and Part adaptors equally. The critical result remains: The Whole advantage did not decrease using the shortened stimuli. This argues against a compound curvature detector explanation but in favor of an inflection-specific shape mechanism.

The inclusion of inflections as a distinct shape feature may aid future models of object recognition and provide a new focus for neurophysiology. Current models of object recognition primarily utilize oriented lines and curves as their "shape primitives" (Barenholtz & Tarr, 2008; Connor, 2004; Hoffman & Richards, 1984; Hoffman & Singh, 1997; Loffler, 2008; Pasupathy & Connor, 2002; Poirier & Wilson, 2006, 2010; Yamane et al., 2008). Inflections are seldom considered in such models despite considerable evidence demonstrating the importance of inflections for vision (Bell, Hancock, et al., 2010; Bertamini & Farrant, 2005; De Winter & Wagemans, 2008; Ivanov & Mullen, 2012; Koenderink, 1984; Koenderink & van Doorn, 1982; Mullen et al., 2011; Richards et al., 1987; Singh & Hoffman, 1999). Our study makes an important addition to this literature by providing the first empirical evidence that the human visual system selectively codes for contour inflections. Further research is required in order to ascertain where inflection coding occurs in the cortical processing hierarchy.

Neurophysiological studies have shown that a variety of contour shapes are represented along the ventral pathway (Gallant, Braun, & Van Essen, 1993; Gallant, Connor, Rakshit, Lewis, & Van Essen, 1996; Lennie, 1998; Schwartz, Desimone, Albright, & Gross, 1983). Recordings from extrastriate cortex in macaques show that in visual area V4, an intermediate area of the form processing pathway, many neurons respond best to contour fragments describing simple curves (Carlson et al., 2011; Pasupathy & Connor, 1999, 2001, 2002), like the single-signed curves represented by the component curves in our Figure 1. Other V4 neurons, however, are selective for fragments describing compound curves, including contours that change in their sign of curvature (Pasupathy & Connor, 1999, 2001), and neurons with similar properties have been recorded in the PIT (Brincat & Connor, 2004, 2006; Yau et al., 2010). These studies provide evidence for mechanisms in V4 and the PIT that selectively code for compound shapes involving multiple curvatures. We suggest that the junction of

two oppositely signed curves, the inflection, represents one specific compound curve that is coded by vision. This is not to say that the contour inflection is the only type of compound curve encoded. The strong aftereffects observed in our Figure 4, following adaptation to the "3" stimulus pair, suggest that there are mechanisms for other specific forms of compound curves. However, we have also clearly shown that only particular forms of compound curves are adaptable. Our final data with RF15 stimuli in Figure 5 show that these compound mechanisms do not extend to arbitrarily complex contours.

Our data also provide some information about the orientation selectivity of the inflection coding mechanisms. We showed in Experiment 3 (Figure 3B) that inflection coding mechanisms are selective for the sign of an inflection as transformed by a reversal in the sign of the amplitude modulation (see Figure 3B inset). However, our data also shows strong transfer to a mirror-symmetric version of an inflection, transformed along its major axis, implying the existence of mechanisms that are selective for a given inflection and its mirror-symmetric counterpart. The latter finding supports a range of studies that have documented the importance of mirror-symmetry in the processing of patterns (Gurnsey, Herbert, & Kenemy, 1998; Wenderoth, 1995), parts of shapes (Bell et al., 2009), and objects (Rhodes et al., 2007; Wilkinson & Halligan, 2002).

Inflections might be coded via an AND-gate operation (e.g., via multiplication or its mathematical equivalent) applied to the responses of neurons detecting two opposite-signed curves in spatial alignment, in line with the suggestion (Poirier & Wilson, 2007) and evidence (Gheorghiu & Kingdom, 2009) that a curve might be coded by AND-gating of its component orientations. The question remains as to whether inflections are processed in parallel with curves or at a different stage in the form processing hierarchy.

Keywords: shape, aftereffects, contour, inflection, curvature

Acknowledgments

This research was supported by an Australian Research Council (ARC) Discovery Project grant #DP110101511 given to J. B., an Irish Research Council Government of Ireland fellowship to D. P. M., and a Natural Sciences and Engineering Research Council of Canada (NSERC) grant #RGPIN 121713-11 given to F. K. We would like to particularly thank James Elder and the anonymous reviewers for their helpful comments on earlier versions of this manuscript.

Commercial relationships: none.
Corresponding author: Jason Bell.
Email: jason.bell@uwa.edu.au.
Address: School of Psychology, University of Western Australia, Crawley, Australia.

References

Barenholtz, E., & Tarr, M. J. (2008). Visual judgment of similarity across shape transformations: Evidence for a compositional model of articulated objects. *Acta Psychologica, 128*(2), 331–338.

Bell, J., & Badcock, D. R. (2009). Narrow-band radial frequency shape channels revealed by sub-threshold summation. *Vision Research*, *49*(8), 843–850.

Bell, J., Badcock, D. R., Wilson, H., & Wilkinson, F. (2007). Detection of shape in radial frequency contours: Independence of local and global form information. *Vision Research*, *47*(11), 1518–1522.

Bell, J., Gheorghiu, E., Hess, R. F., & Kingdom, F. A. A. (2011). Global shape processing involves a hierarchy of integration stages. *Vision Research*, *51*(15), 1760–1766.

Bell, J., Gheorghiu, E., & Kingdom, F. A. A. (2009). Orientation tuning of curvature adaptation reveals both curvature-polarity-selective and non-selective mechanisms. *Journal of Vision*, *9*(12):3, 1–11, http://www.journalofvision.org/content/9/12/3, doi:10.1167/9.12.3. [PubMed] [Article]

Bell, J., Hancock, S., Kingdom, F. A. A., & Peirce, J. W. (2010). Global shape processing: Which parts form the whole? *Journal of Vision*, *10*(6):16, 1–13, http://www.journalofvision.org/content/10/6/16, doi:10.1167/10.6.16. [PubMed] [Article]

Bell, J., Kanji, J., & Kingdom, F. A. A. (2013). Discrimination of rotated-in-depth curves is facilitated by stereoscopic cues, but curvature is not tuned for stereoscopic rotation-in-depth. *Vision Research, 77*, 14–20.

Bell, J., & Kingdom, F. A. A. (2009). Global contour shapes are coded differently from their local components. *Vision Research*, *49*(13), 1702–1710.

Bell, J., Sampasivam, S., McGovern, D., & Kingdom, F. A. A. (2010). More than a simple curve: Evidence for mechanisms which are selective for curves containing inflections. *Journal of Vision, 10*(7):1163, http://www.journalofvision.org/content/10/7/1163, doi:10.1167/10.7.1163. [Abstract]

Bertamini, M., & Farrant, T. (2005). Detection of change in shape and its relation to part structure. *Acta Psychologica*, *120*(1), 35–54.

Brincat, S. L., & Connor, C. E. (2004). Underlying principles of visual shape selectivity in posterior inferotemporal cortex. *Nature Neuroscience*, *7*(8), 880–886.

Brincat, S. L., & Connor, C. E. (2006). Dynamic shape synthesis in posterior inferotemporal cortex. *Neuron, 49*(1), 17–24.

Carlson, E. T., Rasquinha, R. J., Zhang, K., & Connor, C. E. (2011). A sparse object coding scheme in area V4. *Current Biology, 21*(4), 288–293.

Chatila, J., & Tabbara, M. (2004). Computational modeling of flow over an ogee spillway. *Computers & Structures*, *82*(22), 1805–1812.

Connor, C. E. (2004). Shape dimensions and object primitives. In L. M. Chalupa & J. S. Werner (Eds.), *The visual neurosciences* (pp. 1080–1089). London: MIT Press.

De Winter, J., & Wagemans, J. (2008). The awakening of Attneave's sleeping cat: Identification of everyday objects on the basis of straight-line versions of outlines. *Perception, 37*(2), 245–270.

Elder, J. H., & Goldberg, R. M. (2002). Ecological statistics of Gestalt laws for the perceptual organization of contours. *Journal of Vision*, *2*(4):5, 324–353, http://www.journalofvision.org/content/2/4/5, doi:10.1167/2.4.5. [PubMed] [Article]

Ewing, G. M. (1938). On the definition of inflection point. *The American Mathematical Monthly*, *45*(10), 681–683.

Faroqi-Shah, Y., & Thompson, C. K. (2007). Verb inflections in agrammatic aphasia: Encoding of tense features. *Journal of Memory and Language, 56*(1), 129–151.

Faroqi-Shah, Y., & Thompson, C. K. (2010). Production latencies of morphologically simple and complex verbs in aphasia. *Clinical Linguistics & Phonetics*, *24*(12), 963–979.

Gallant, J. L., Braun, J., & Van Essen, D. C. (1993). Selectivity for polar, hyperbolic, and Cartesian gratings in macaque visual cortex. *Science*, *259*(5091), 100–103.

Gallant, J. L., Connor, C. E., Rakshit, S., Lewis, J. W., & Van Essen, D. C. (1996). Neural responses to polar, hyperbolic, and Cartesian gratings in area V4 of the macaque monkey. *Journal of Neurophysiology*, *76*(4), 2718–2739.

Geisler, W. S., Perry, J. S., Super, B. J., & Gallogly, D. P. (2001). Edge co-occurrence in natural images predicts contour grouping performance. *Vision Research*, *41*(6), 711–724.

Gheorghiu, E., & Kingdom, F. A. (2006). Luminance-contrast properties of contour-shape processing revealed through the shape-frequency after-effect. *Vision Research*, *46*(21), 3603–3615.

Gheorghiu, E., & Kingdom, F. A. (2007). The spatial feature underlying the shape-frequency and shape-amplitude after-effects. *Vision Research*, *47*(6), 834–844.

Gheorghiu, E., & Kingdom, F. A. (2009). Multiplication in curvature processing. *Journal of Vision*, *9*(2): 23, 1–17, http://www.journalofvision.org/content/9/2/23, doi:10.1167/9.2.23. [PubMed] [Article]

Gibson, J. J., & Radner, M. (1937). Adaptation, after-effect and contrast in the perception of tilted lines. *Journal of Experimental Psychology, 20,* 453–467.

Gurnsey, R., Herbert, A. M., & Kenemy, J. (1998). Bilateral symmetry embedded in noise is detected accurately only at fixation. *Vision Research*, *38*(23), 3795–3803.

Hancock, S., McGovern, D. P., & Peirce, J. W. (2010). Ameliorating the combinatorial explosion with spatial frequency-matched combinations of V1 outputs. *Journal of Vision*, *10*(8):7, 1–14, http://www.journalofvision.org/content/10/8/7, doi:10.1167/10.8.7. [PubMed] [Article]

Hancock, S., & Peirce, J. W. (2008). Selective mechanisms for simple contours revealed by compound adaptation. *Journal of Vision, 8*(7):11, 1–10, http://www.journalofvision.org/content/8/7/11, doi:10.1167/8.7.11. [PubMed] [Article]

Hoffman, D. D., & Richards, W. A. (1984). Parts of recognition. *Cognition, 18*(1–3), 65–96.

Hoffman, D. D., & Singh, M. (1997). Salience of visual parts. *Cognition*, *63*(1), 29–78.

Hubel, D. H., & Wiesel, T. N. (1962). Receptive fields, binocular interaction and functional architecture in the cat's visual cortex. *The Journal of Physiology, 160,* 106–154.

Hubel, D. H., & Wiesel, T. N. (1968). Receptive fields and functional architecture of monkey striate cortex. *The Journal of Physiology, 195*(1), 215–243.

Irwin, F., & Wright, H. N. (1917). Some properties of polynomial curves. *Annals of Mathematics*, *19*(2), 152–158.

Ivanov, I. V., & Mullen, K. T. (2012). The role of local features in shape discrimination of contour- and surface-defined radial frequency patterns at low contrast. *Vision Research*, *52*(1), 1–10.

Jahnkassim, P. S. (2002). The 'curves of nature': The organic inflections of modern regionalism and ecological architecture in an urbanising context. In C. A. Brebbia, L. J. Sucharov, & P. Pascolo (Eds.), *Designs and nature: Comparing design in nature with science* (pp 236–244). Southampton: WIT Press.

Jeffrey, B. G., Wang, Y. Z., & Birch, E. E. (2002). Circular contour frequency in shape discrimination. *Vision Research*, *42*(25), 2773–2779.

Kapadia, M. K., Westheimer, G., & Gilbert, C. D.

(1999). Dynamics of spatial summation in primary visual cortex of alert monkeys. *Proceedings of the National Academy of Sciences, USA, 96*(21), 12073–12078.

Kapadia, M. K., Westheimer, G., & Gilbert, C. D. (2000). Spatial distribution of contextual interactions in primary visual cortex and in visual perception. *Journal of Neurophysiology*, *84*(4), 2048–2062.

Koenderink, J. J. (1984). What does the occluding contour tell us about solid shape. *Perception*, *13*(3), 321–330.

Koenderink, J. J., & van Doorn, A. J. (1982). The shape of smooth objects and the way contours end. *Perception*, *11*(2), 129–137.

Lennie, P. (1998). Single units and visual cortical organization. *Perception*, *27*(8), 889–935.

Loffler, G. (2008). Perception of contours and shapes: Low and intermediate stage mechanisms. *Vision Research*, *48*(20), 2106–2127.

Loffler, G., Wilson, H. R., & Wilkinson, F. (2003). Local and global contributions to shape discrimination. *Vision Research*, *43*(5), 519–530.

Magnussen, S., & Kurtenbach, W. (1979). A test for contrast-polarity selectivity in the tilt aftereffect. *Perception*, *8*(5), 523–528.

McGovern, D. P., Hancock, S., & Peirce, J. W. (2011). The timing of binding and segregation of two compound aftereffects. *Vision Research*, *51*(9), 1047–1057.

McGovern, D. P., & Peirce, J. W. (2010). The spatial characteristics of plaid-form-selective mechanisms. *Vision Research*, *50*(8), 796–804.

Mullen, K. T., Beaudot, W. H. A., & Ivanov, I. V. (2011). Evidence that global processing does not limit thresholds for RF shape discrimination. *Journal of Vision*, *11*(3):6, 1–21, http://www.journalofvision.org/content/11/3/6, doi:10.1167/11.3.6. [PubMed] [Article]

Muller, K. M., Wilke, M., & Leopold, D. A. (2009). Visual adaptation to convexity in macaque area V4. *Neuroscience*, *161*(2), 655–662.

Pasupathy, A., & Connor, C. E. (1999). Responses to contour features in macaque area V4. *Journal of Neurophysiology*, *82*(5), 2490–2502.

Pasupathy, A., & Connor, C. E. (2001). Shape representation in area V4: Position-specific tuning for boundary conformation. *Journal of Neurophysiology, 86*(5), 2505–2519.

Pasupathy, A., & Connor, C. E. (2002). Population coding of shape in area V4. *Nature Neuroscience*, *5*(12), 1332–1338.

Peirce, J. W., & Taylor, L. J. (2006). Selective mechanisms for complex visual patterns revealed by adaptation. *Neuroscience*, *141*(1), 15–18.

Poirier, F. J. A. M., & Wilson, H. R. (2006). A biologically plausible model of human radial frequency perception. *Vision Research*, *46*(15), 2443–2455.

Poirier, F. J. A. M., & Wilson, H. R. (2007). Object perception and masking: Contributions of sides and convexities. *Vision Research, 47*(23), 3001–3011.

Poirier, F. J. A. M., & Wilson, H. R. (2010). A biologically plausible model of human shape symmetry perception. *Journal of Vision*, *10*(1):9, 1–16, http://www.journalofvision.org/content/10/1/9, doi:10.1167/10.1.9. [PubMed] [Article]

Rhodes, G., Yoshikawa, S., Palermo, R., Simmons, L. W., Peters, M., Lee, K., ... Crawford, J. R. (2007). Perceived health contributes to the attractiveness of facial symmetry, averageness, and sexual dimorphism. *Perception, 36*(8), 1244–1252.

Richards, W. A., Koenderink, J. J., & Hoffman, D. D. (1987). Inferring three-dimensional shapes from two-dimensional silhouettes. *Journal of the Optical Society of America A*, *4*(7), 1168–1175.

Schwartz, E. L., Desimone, R., Albright, T. D., & Gross, C. G. (1983). Shape recognition and inferior temporal neurons. *Proceedings of the National Academy of Sciences, USA, 80*(18), 5776–5778.

Singh, M., & Hoffman, D. D. (1999). Completing visual contours: The relationship between relatability and minimizing inflections. *Perception & Psychophysics, 61*(5), 943–951.

Wenderoth, P. (1995). The role of pattern outline in bilateral symmetry detection with briefly flashed dot patterns. *Spat Vis*, *9*(1), 57–77.

Wilkinson, D. T., & Halligan, P. W. (2002). The effects of stimulus symmetry on landmark judgments in left and right visual fields. *Neuropsychologia*, *40*(7), 1045–1058.

Wilkinson, F., Wilson, H. R., & Habak, C. (1998). Detection and recognition of radial frequency patterns. *Vision Research*, *38*(22), 3555–3568.

Yamane, Y., Carlson, E. T., Bowman, K. C., Wang, Z., & Connor, C. E. (2008). A neural code for three-dimensional object shape in macaque inferotemporal cortex. *Nature Neuroscience*, *11*(11), 1352–1360.

Yau, J., Pasupathy, A., Brincat, S., & Connor, C. (2010). Dynamic synthesis of curvature in area V4. *Journal of Vision, 10*(7):911, http://www.journalofvision.org/content/10/7/911, doi:10.1167/10.7.911. [Abstract]